

SUPPLEMENTAL MATERIAL: Model Code, Supplemental Figures and Tables

Thorough QT/QTc in a Dish: An In Vitro Human Model That Accurately Predicts Clinical Concentration-QTc Relationships

Alexander D. Blanchette, BS^{1*}; Fabian A. Grimm, PhD^{1*}; Chimedullam Dalaijamts, PhD¹; Nan-Hung Hsieh, PhD¹; Kyle Ferguson, MS¹; Yu-Syuan Luo, PhD¹; Ivan Rusyn, MD PhD¹; Weihsueh A. Chiu, PhD¹

¹Department of Veterinary Integrative Biosciences, Texas A&M University, College Station, TX

* These authors equally contributed to this manuscript

Address correspondence to:

Weihsueh A. Chiu, PhD, Department of Veterinary Integrative Biosciences, 4458 TAMU, Texas A&M University, College Station, TX 77843, (979) 845-4106, fax: (979) 847-8981

Conflict of Interest Statement

The authors declared no competing interests for this work.

Bayesian Dose-Response Model (stan version 2.17.3(1))

```
data {
    real scale_factor; // overall scaling factor
    int<lower=0> Ni; // Number of cell lines
    int<lower=0> Nj; // Number of data points
    vector[Nj] x; // concentrations
    vector[Nj] ys; // responses, scaled by scale_factor
    int<lower=0,upper=Ni> cell[Nj]; // cell line for each data point
    int<lower=1> Nquants; // Number of quantiles of EC10 to calculate
    vector[Nquants] quants; // Quantiles (e.g.,
    c(0.01,0.025,0.5,0.975,0.99))
}
parameters {
    // Population mean
    real m_y0; // background
    real m_x0; // numerator scale
    real m_Emax; // max effect size
    real m_n; // Hill exponent
    // Population standard deviation
    real<lower=0> sd_y0;
    real<lower=0> sd_x0;
    real<lower=0> sd_Emax;
    real<lower=0> sd_n;
    // Inter-individual variability
    real z_y0[Ni];
    real z_x0[Ni];
    real z_Emax[Ni];
    real z_n[Ni];
    // Residual error variance
    real<lower=0> sigma_y;
}
transformed parameters {
    real y0[Ni]; // untransformed background
    real x0[Ni]; // untransformed numerator scale
    real Emax[Ni]; // untransformed max effect size
    real n[Ni]; // untransformed Hill exponent
    for (i in 1:Ni) { // un-log transform
        y0[i] = exp(m_y0 + sd_y0 * z_y0[i]);
        x0[i] = exp(m_x0 + sd_x0 * z_x0[i]);
        Emax[i] = exp(m_Emax + sd_Emax * z_Emax[i]); // Emax
    }
    positive
        n[i] = exp(m_n + sd_n * z_n[i]);
    }
model {
```

```

vector[Nj] yp;
// prior distributions
m_y0 ~ normal(0,5);
m_x0 ~ normal(0,5);
m_Emax ~ normal(0,5);
m_n ~ normal(0,1);
sd_y0 ~ normal(0,1);
sd_x0 ~ normal(0,1);
sd_Emax ~ normal(0,1);
sd_n ~ normal(0,0.2);
z_y0 ~ normal(0,1);
z_x0 ~ normal(0,1);
z_Emax ~ normal(0,1);
z_n ~ normal(0,1);
sigma_y ~ normal(0,0.2);
for (j in 1:Nj) {
    yp[j] = y0[cell[j]]*(1 + (x[j] / x0[cell[j]])^n[cell[j]] /
(1 + ((x[j] / x0[cell[j]])^n[cell[j]])/Emax[cell[j]]));
}
ys ~ student_t(5,yp,sigma_y);
}
generated quantities {
    vector[Ni] ec10;      // Concentration at which the relative
response is 10%
    for (i in 1:Ni) {
        if (Emax[i] > 0.1)
            ec10[i] = x0[i]*(0.1 * Emax[i] / (Emax[i] -
0.1))^(1/n[i]);
        else
            ec10[i] = 1000;
    }
}

```

SUPPLEMENTAL FIGURES AND FIGURE LEGENDS

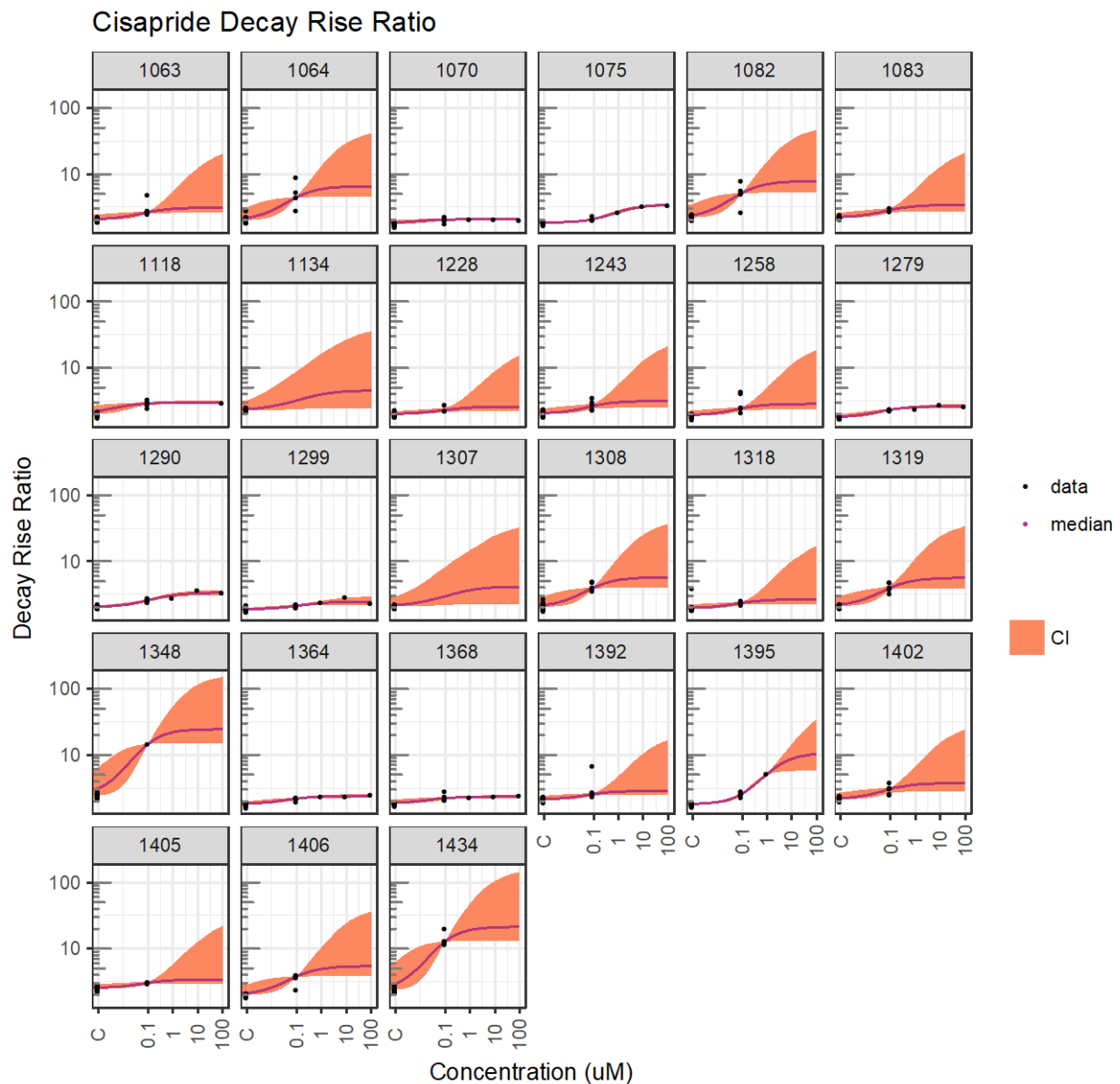


Figure S1. Concentration-response model fits for cisapride showing decay-rise data (black dots); median prediction (colored lines) and 95% CI (colored shadings). Each panel is a different donor.

Citalopram Decay Rise Ratio

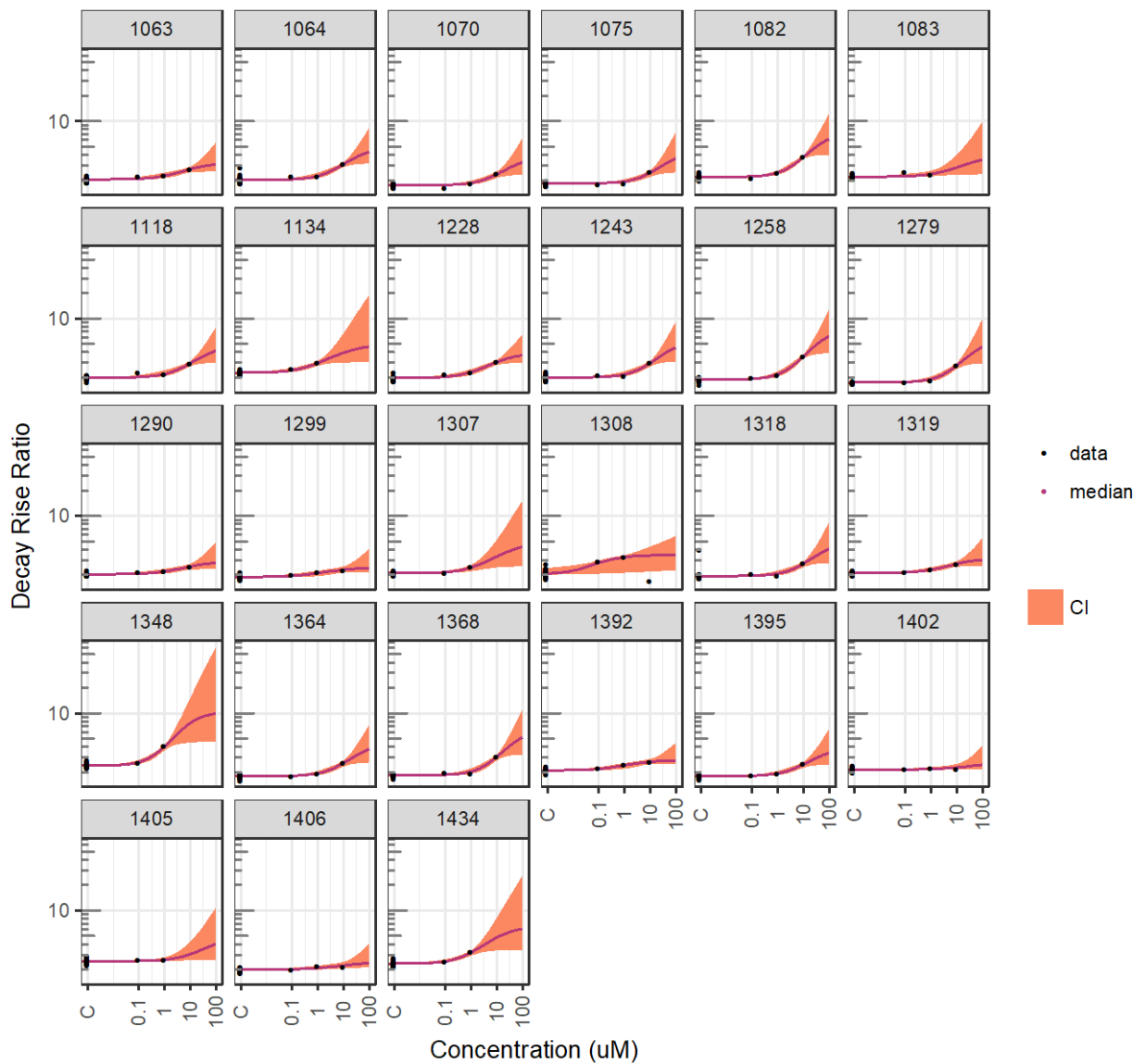


Figure S2. Concentration-response model fits for citalopram showing decay-rise data (black dots); median prediction (colored lines) and 95% CI (colored shadings). Each panel is a different donor.

Disopyramide Decay Rise Ratio

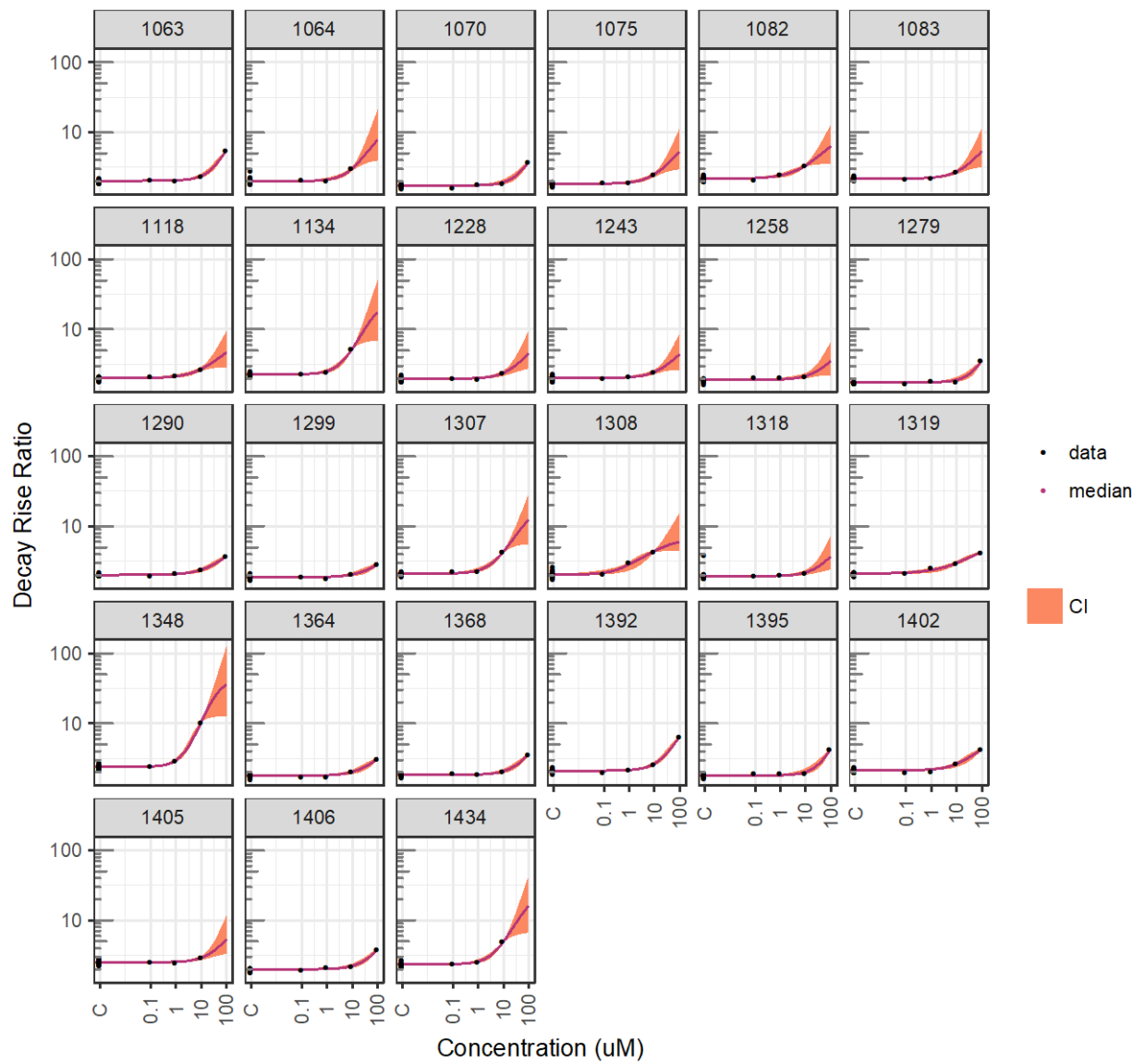


Figure S3. Concentration-response model fits for disopyramide showing decay-rise data (black dots); median prediction (colored lines) and 95% CI (colored shadings). Each panel is a different donor.

Dofetilide Decay Rise Ratio

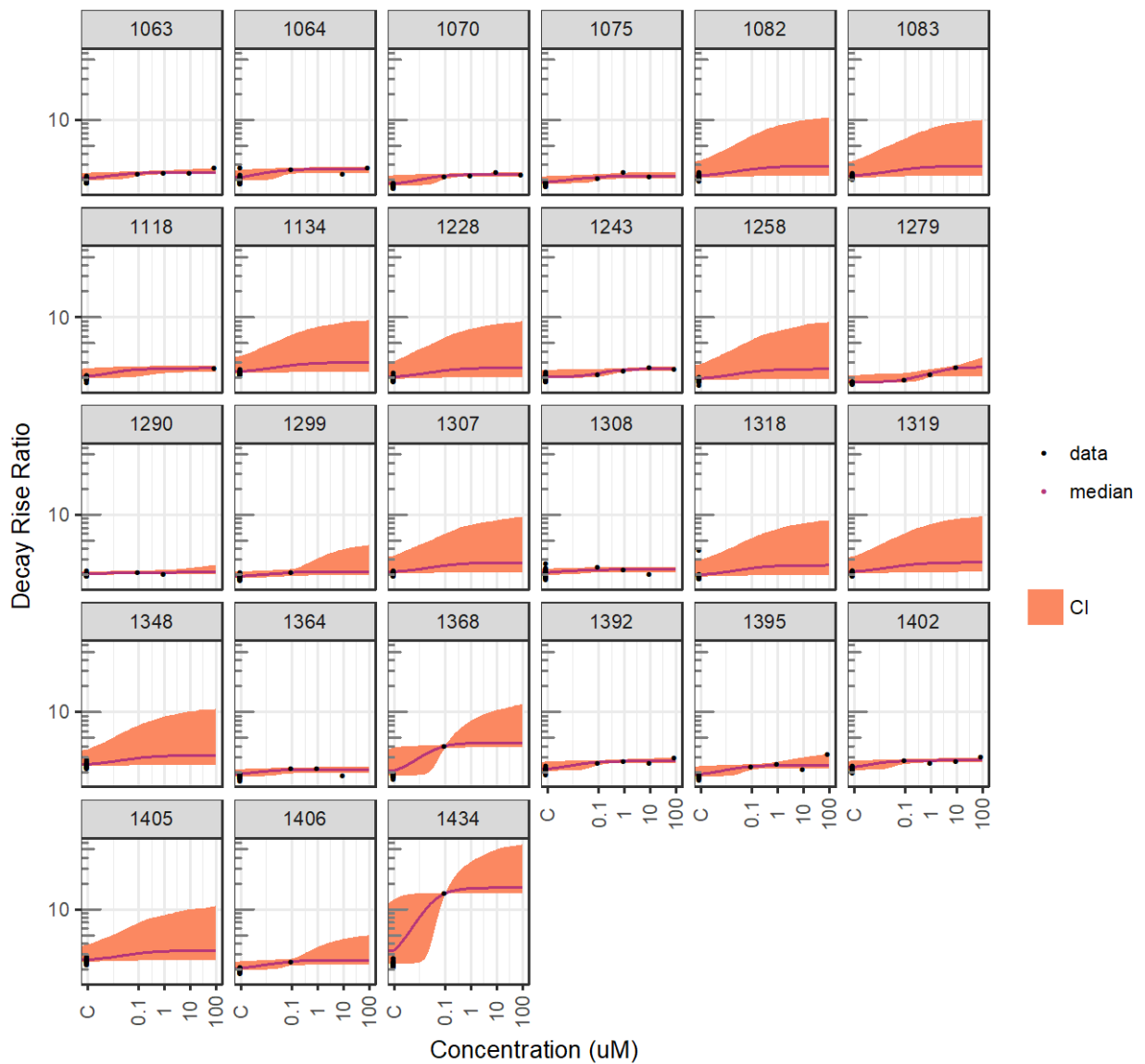


Figure S4. Concentration-response model fits for dofetilide showing decay-rise data (black dots); median prediction (colored lines) and 95% CI (colored shadings). Each panel is a different donor.

Moxifloxacin Decay Rise Ratio

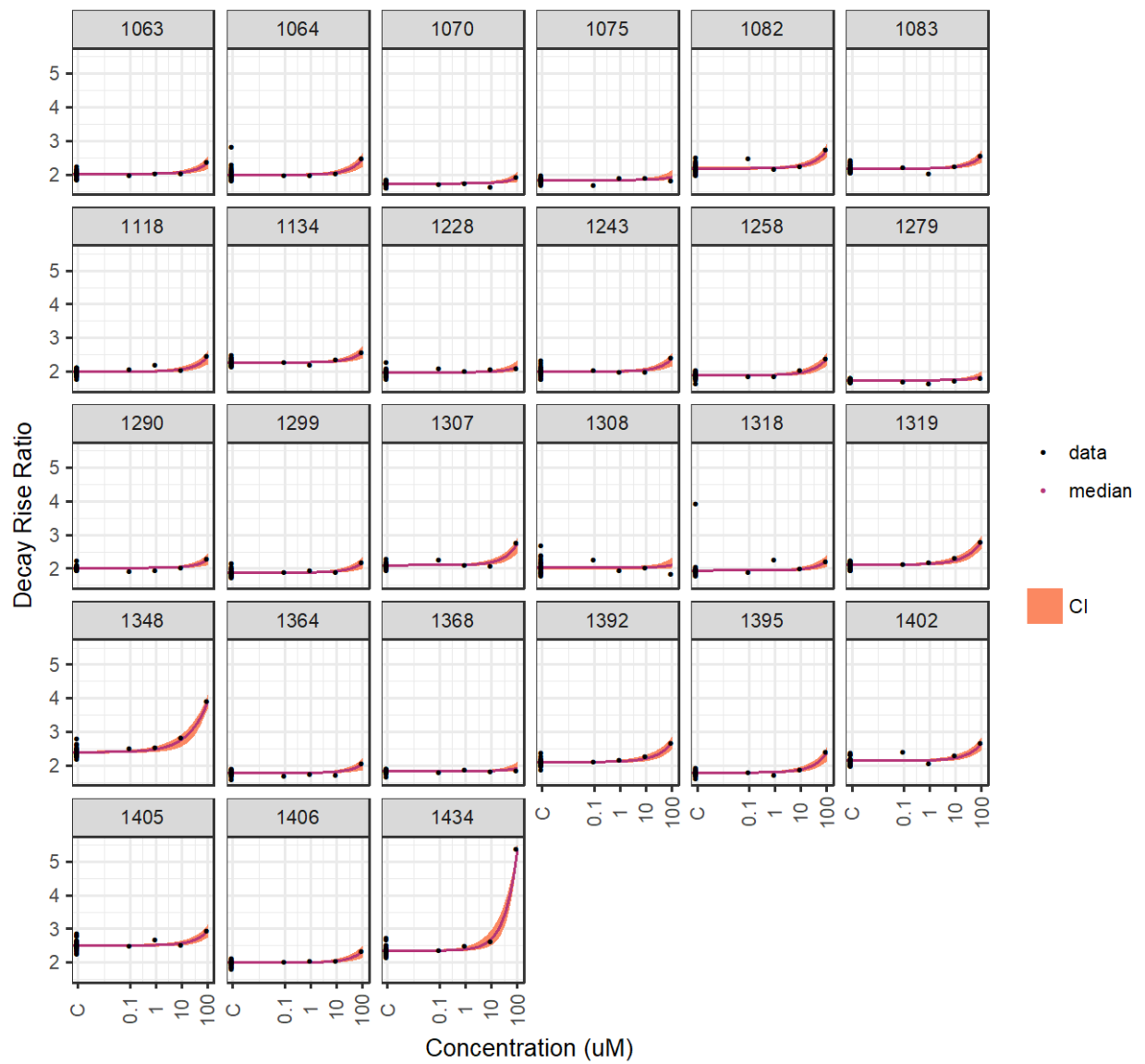


Figure S5. Concentration-response model fits for moxifloxacin showing decay-rise data (black dots); median prediction (colored lines) and 95% CI (colored shadings). Each panel is a different donor.

N-acetylprocainamide Decay Rise Ratio

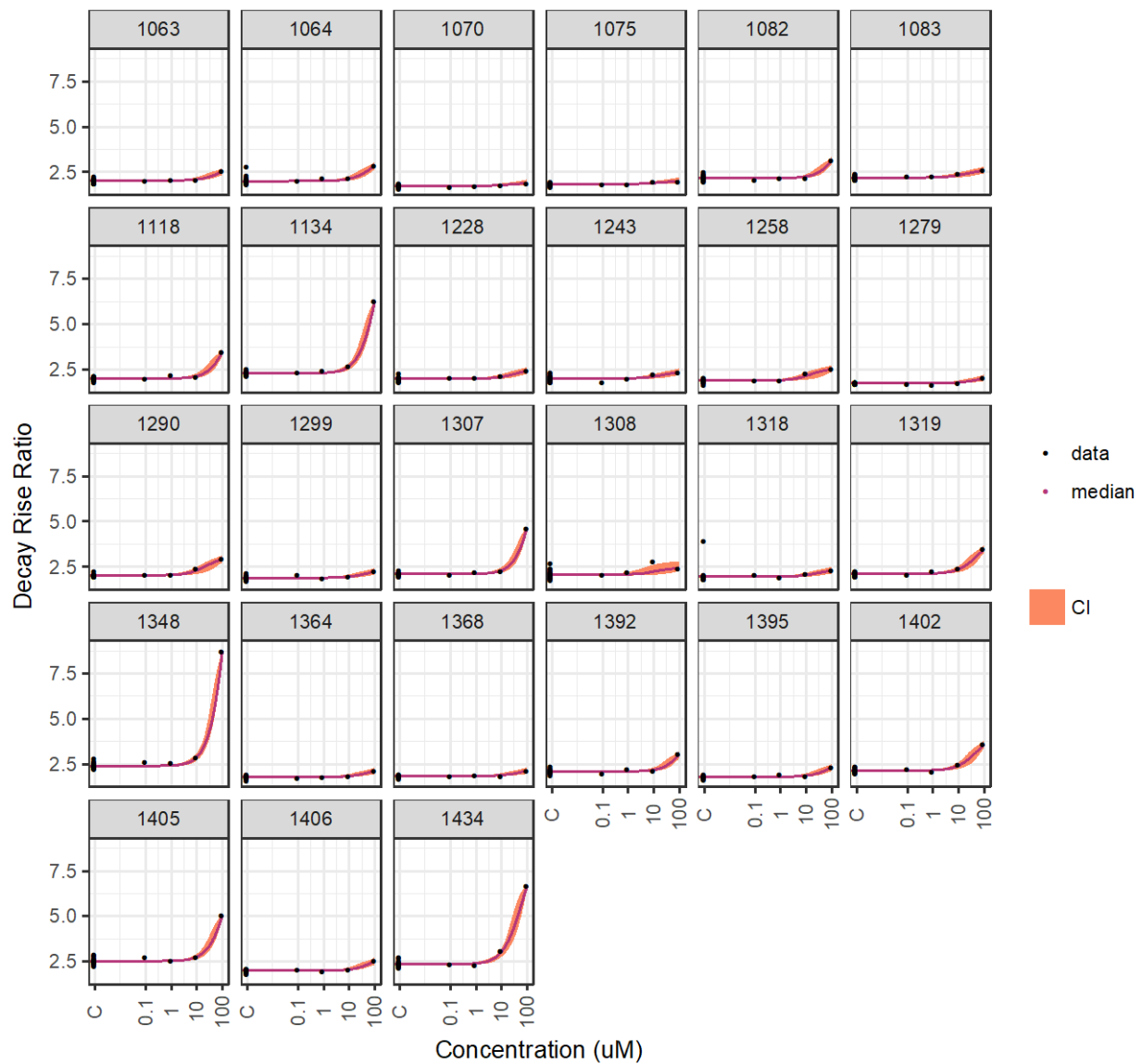


Figure S6. Concentration-response model fits for N-acetylprocainamide showing decay-rise data (black dots); median prediction (colored lines) and 95% CI (colored shadings). Each panel is a different donor.

Quinidine Decay Rise Ratio

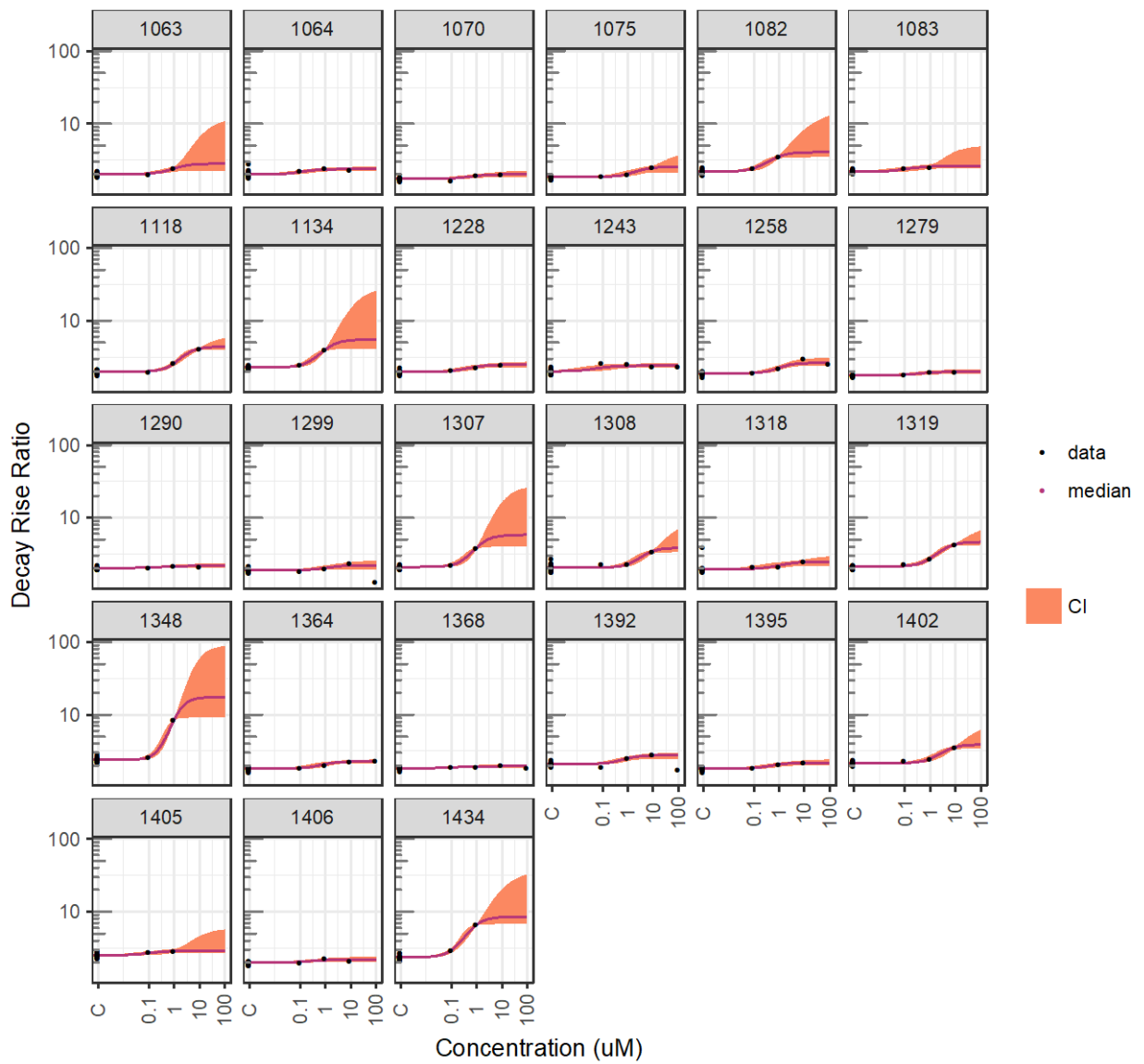


Figure S7. Concentration-response model fits for quinidine showing decay-rise data (black dots); median prediction (colored lines) and 95% CI (colored shadings). Each panel is a different donor.

Sematilide Decay Rise Ratio

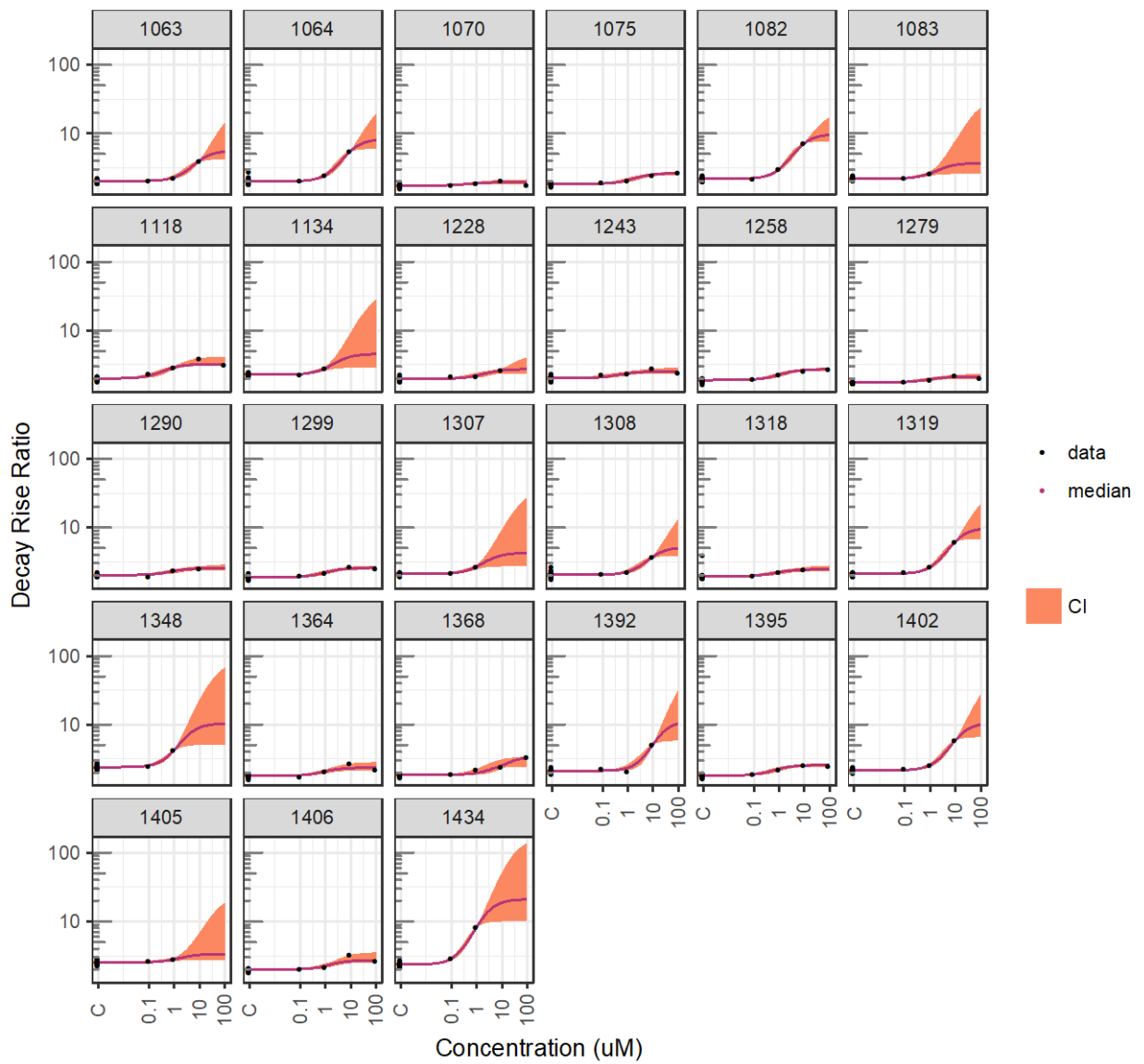


Figure S8. Concentration-response model fits for sematilide showing decay-rise data (black dots); median prediction (colored lines) and 95% CI (colored shadings). Each panel is a different donor.

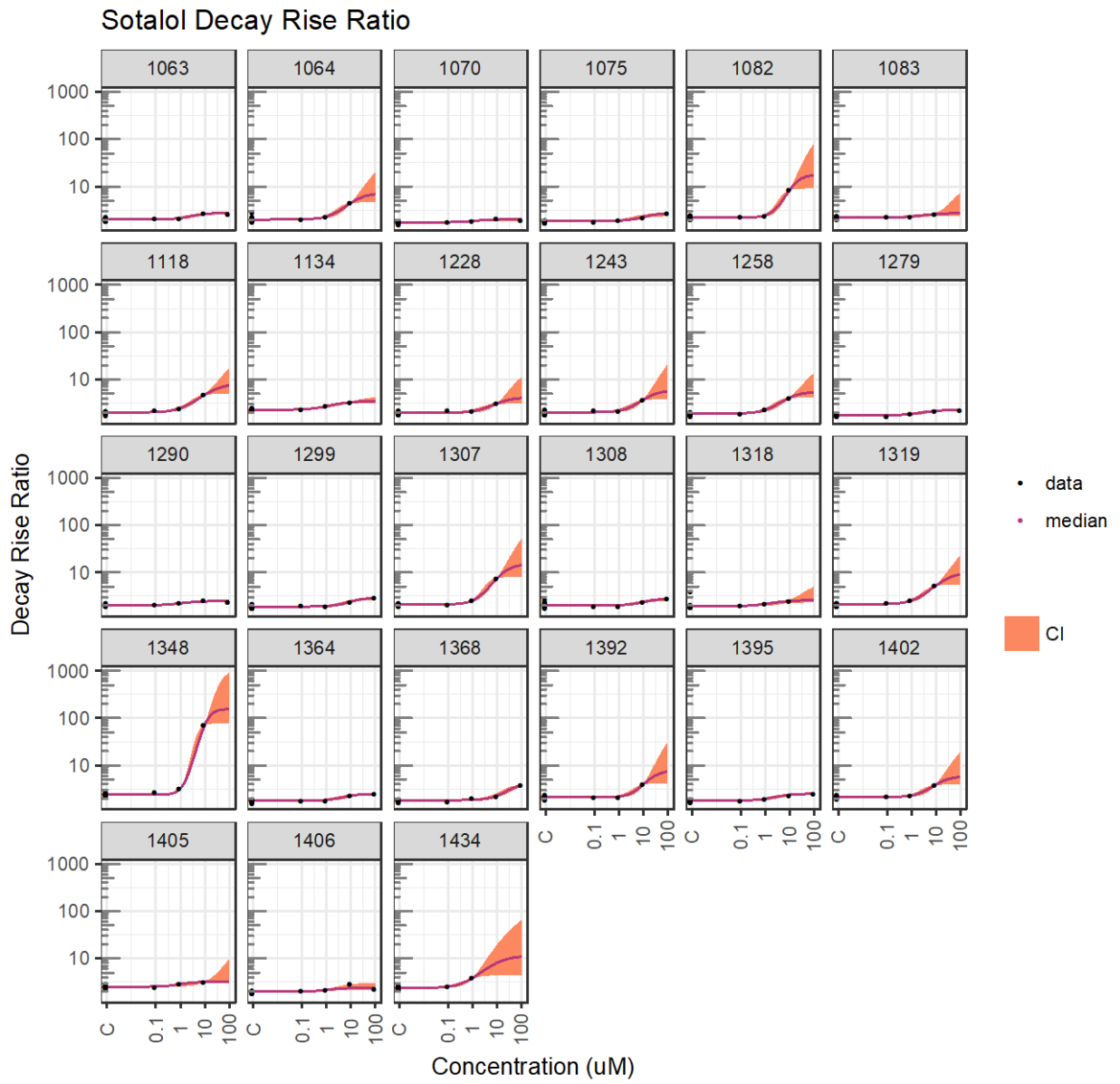


Figure S9. Concentration-response model fits for sotalol showing decay-rise data (black dots); median prediction (colored lines) and 95% CI (colored shadings). Each panel is a different donor.

Vernacalant Decay Rise Ratio

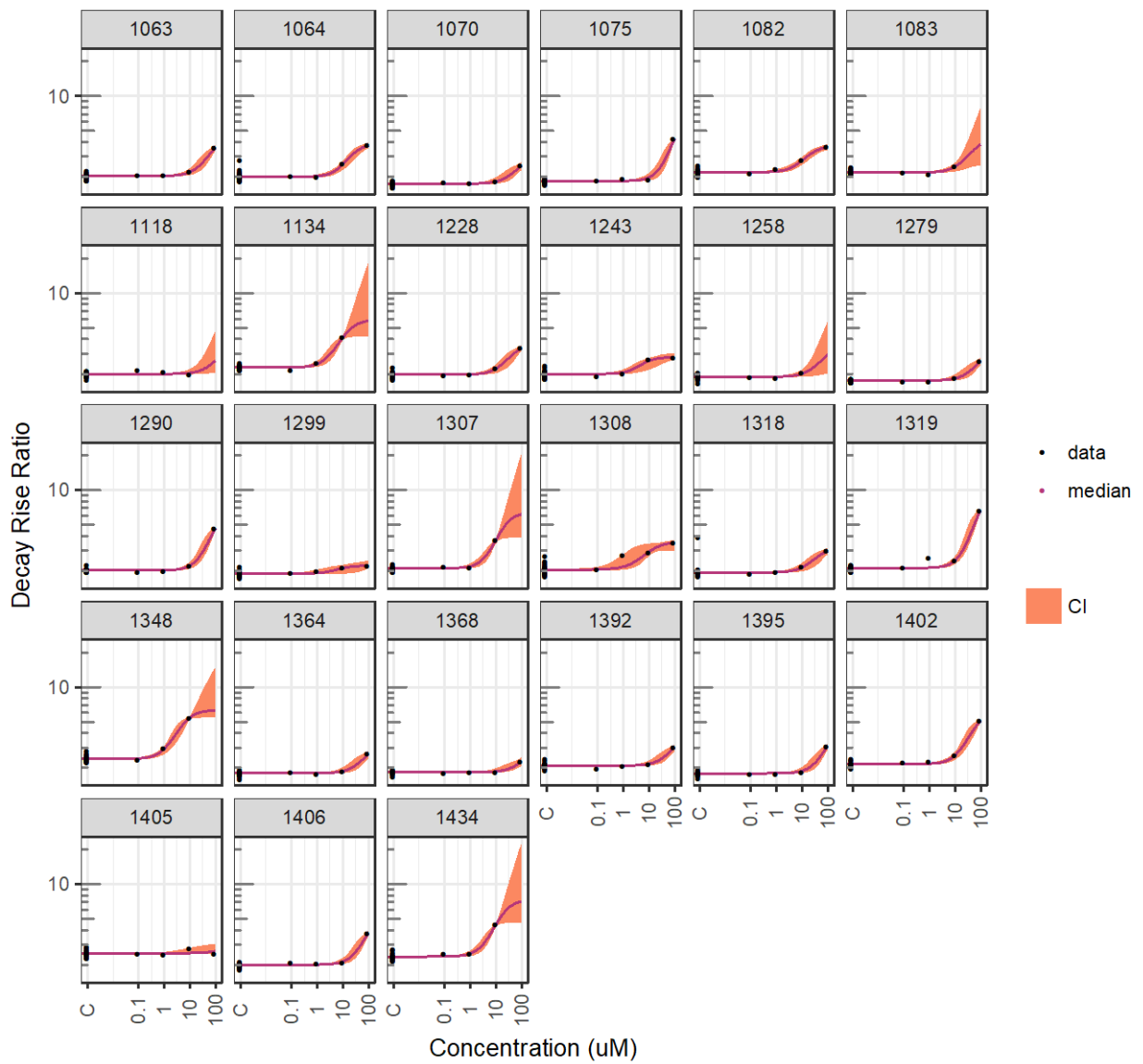


Figure S10. Concentration-response model fits for vernacalant showing decay-rise data (black dots); median prediction (colored lines) and 95% CI (colored shadings). Each panel is a different donor.

Cabazitaxel Decay Rise Ratio

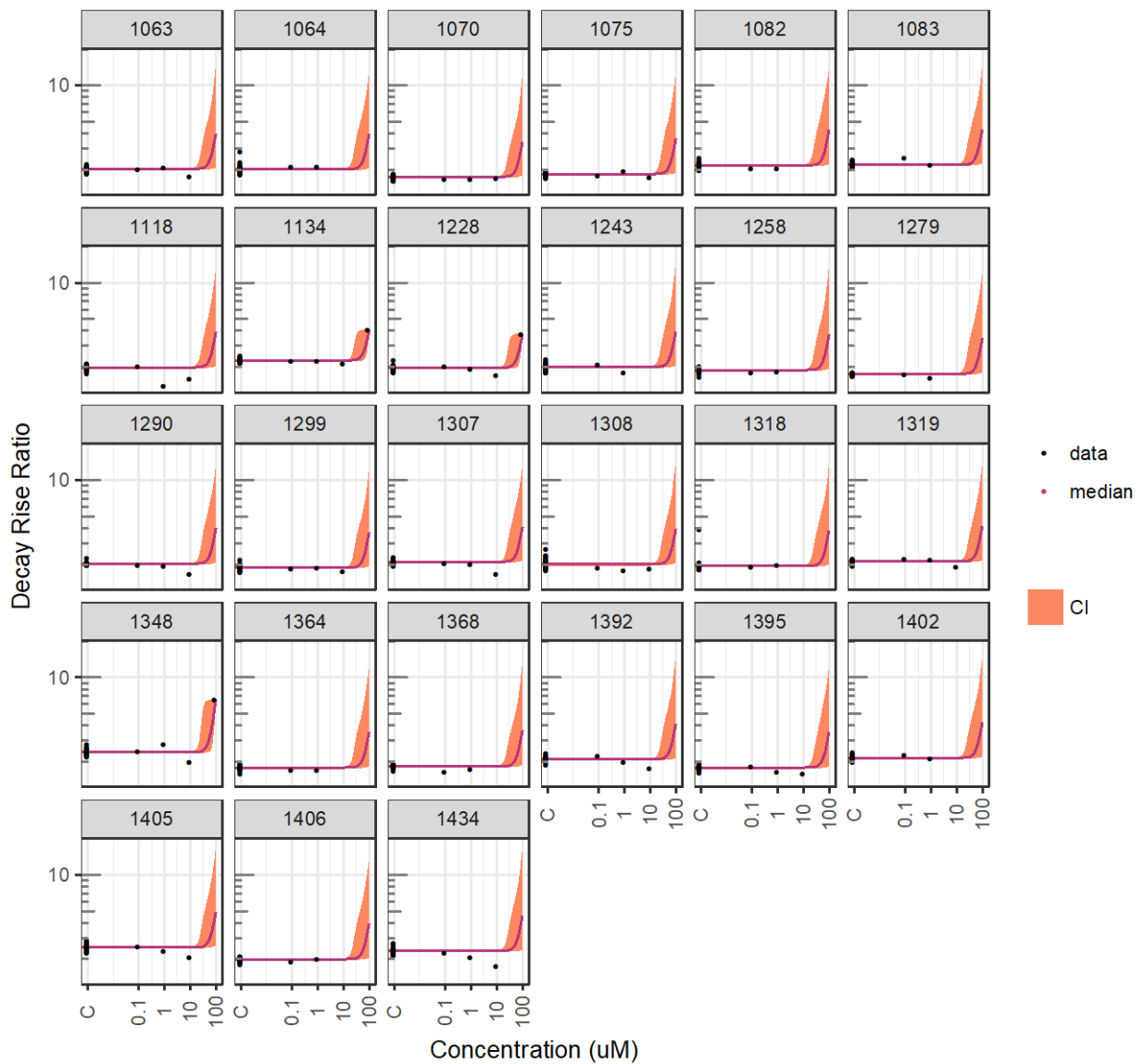


Figure S11. Concentration-response model fits for cabazitaxel showing decay-rise data (black dots); median prediction (colored lines) and 95% CI (colored shadings). Each panel is a different donor.

Lamotrigine Decay Rise Ratio

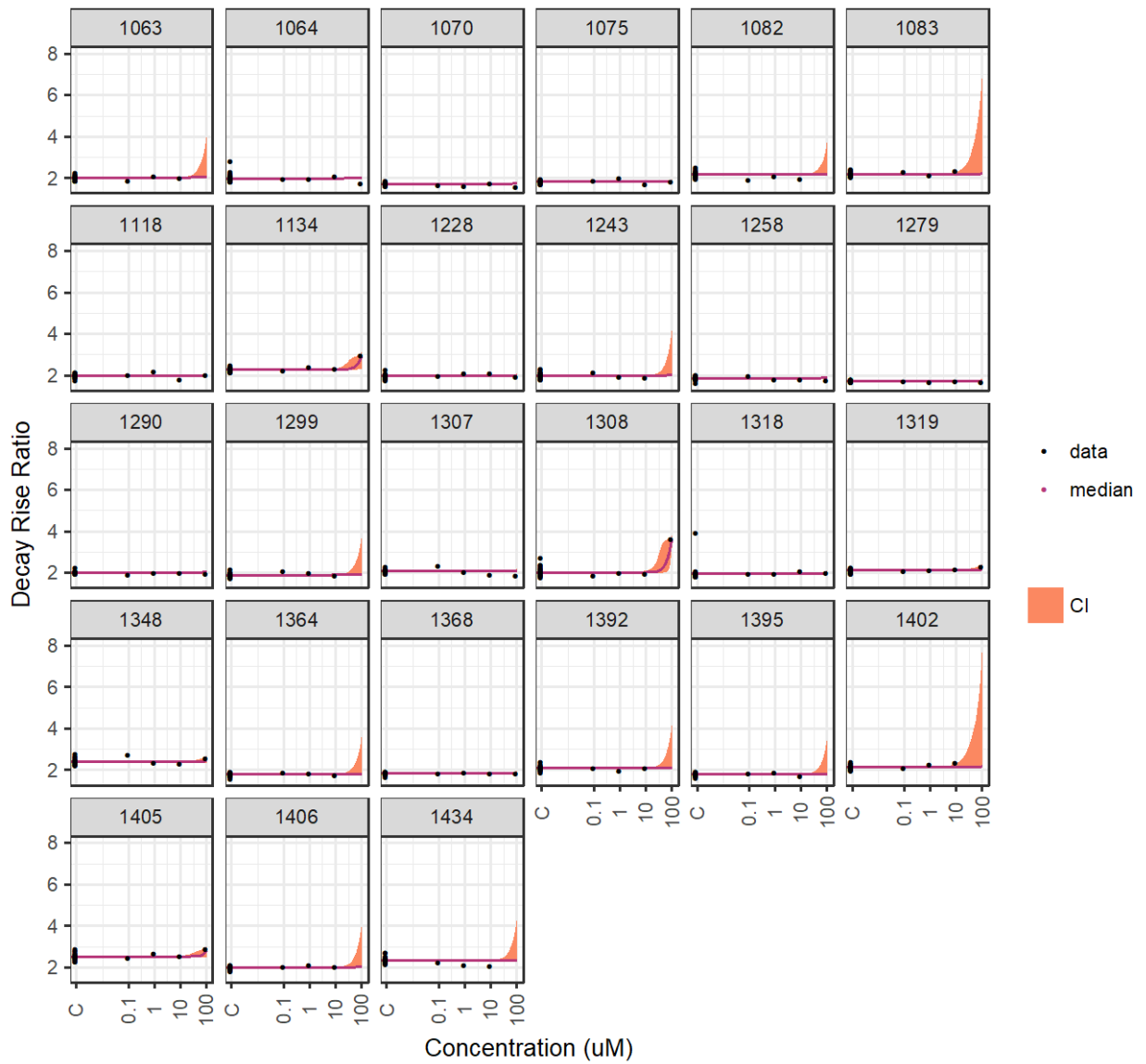


Figure S12. Concentration-response model fits for lamotrigine showing decay-rise data (black dots); median prediction (colored lines) and 95% CI (colored shadings). Each panel is a different donor.

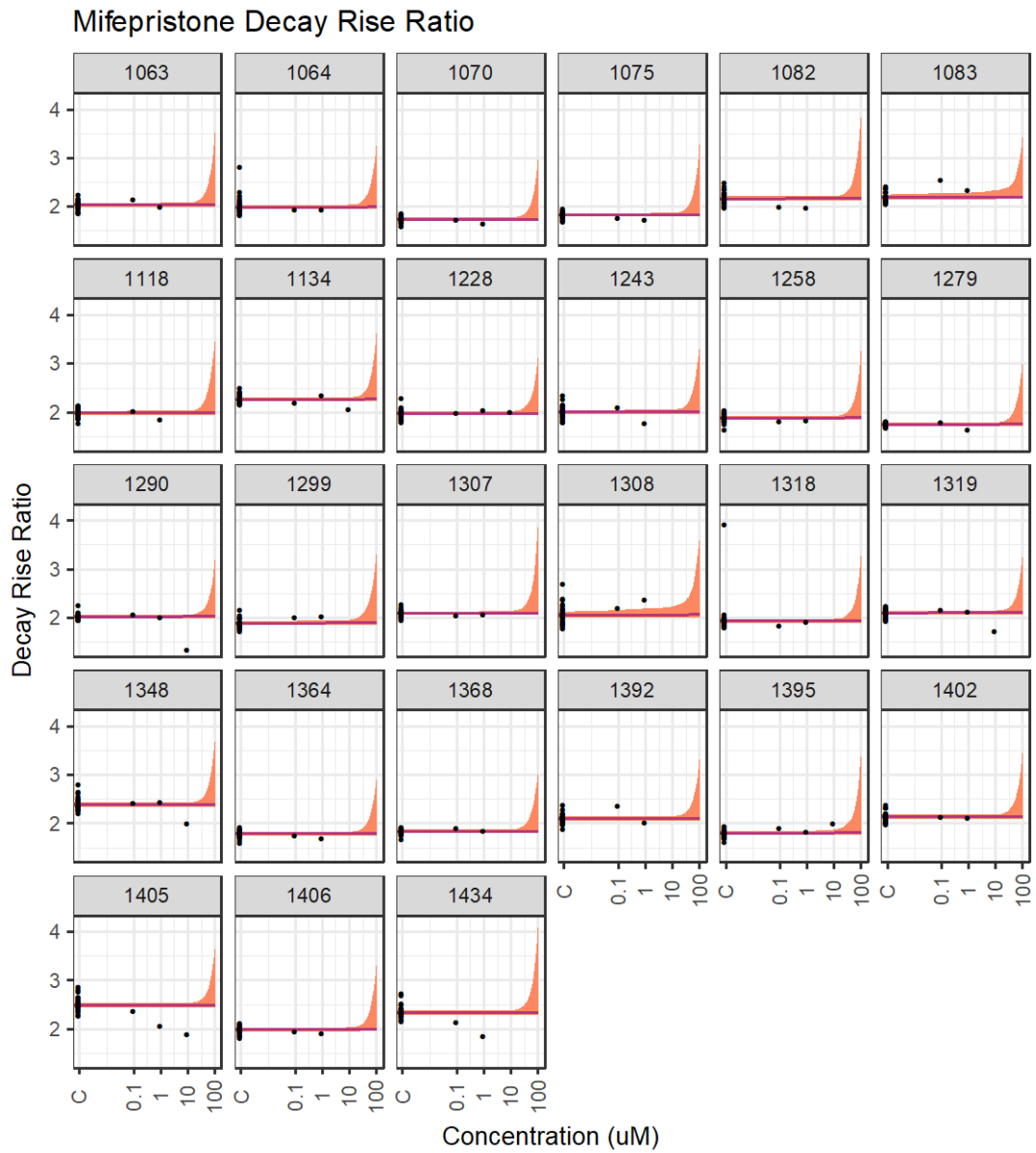


Figure S13. Concentration-response model fits for mifepristone showing decay-rise data (black dots); median prediction (colored lines) and 95% CI (colored shadings). Each panel is a different donor.

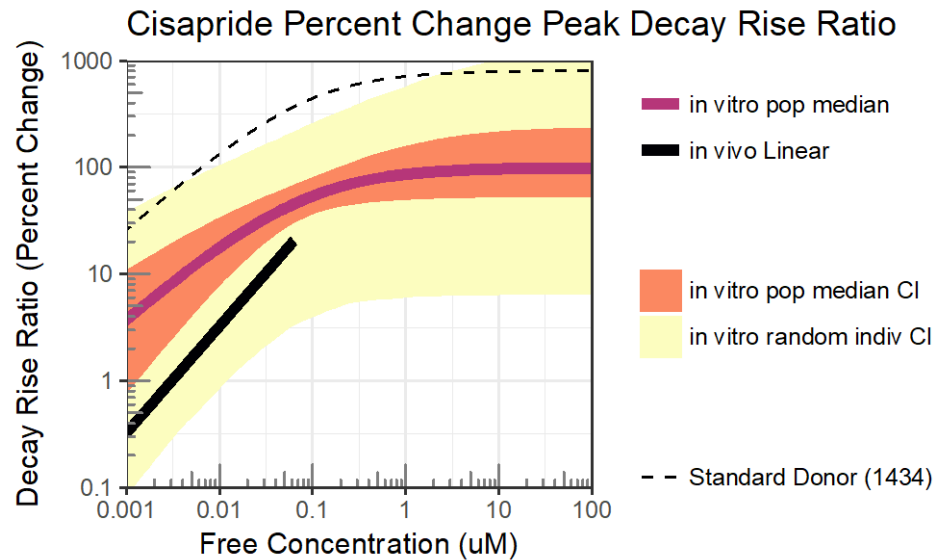


Figure S14. Comparison of cisapride concentration-response functions based on *in vivo* data (black line) compared to *in vitro* data (magenta line: population median; orange region: 95% confidence interval on population median; yellow region: 95% confidence interval on random individual; dashed line: standard iCell donor (1434).

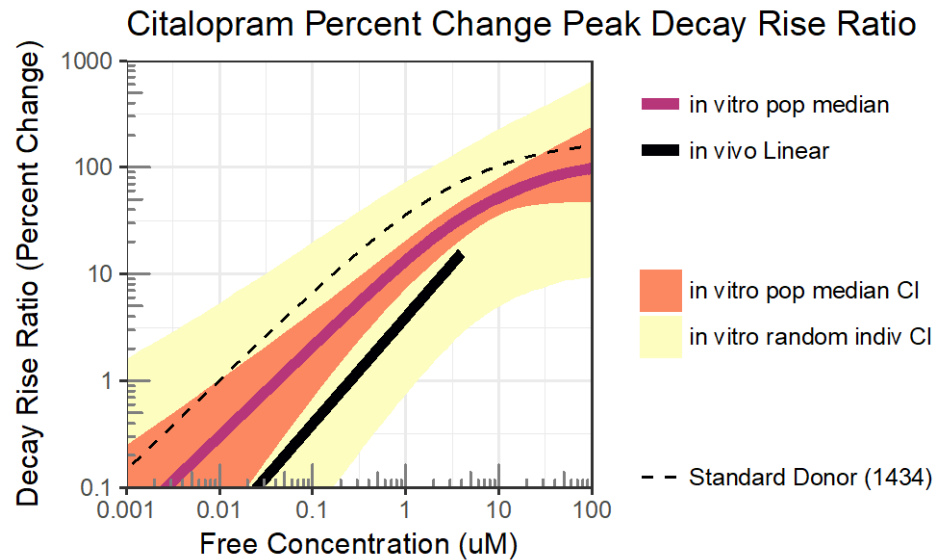


Figure S15. Comparison of citalopram concentration-response functions based on *in vivo* data (black line) compared to *in vitro* data (magenta line: population median; orange region: 95% confidence interval on population median; yellow region: 95% confidence interval on random individual; dashed line: standard iCell donor (1434)).

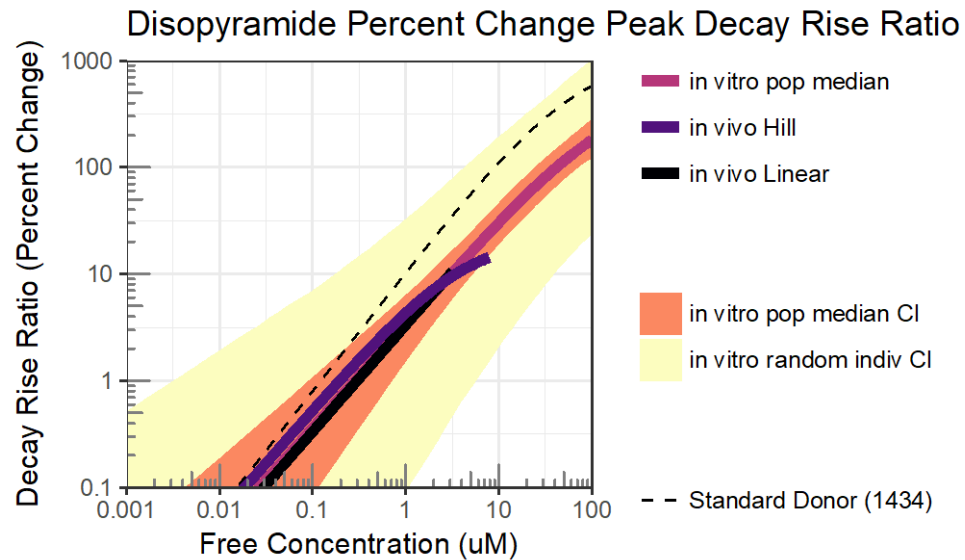


Figure S16. Comparison of disopyramide concentration-response functions based on *in vivo* data (black line [linear]; purple line [Hill]) compared to *in vitro* data (magenta line: population median; orange region: 95% confidence interval on population median; yellow region: 95% confidence interval on random individual; dashed line: standard iCell donor (1434)).

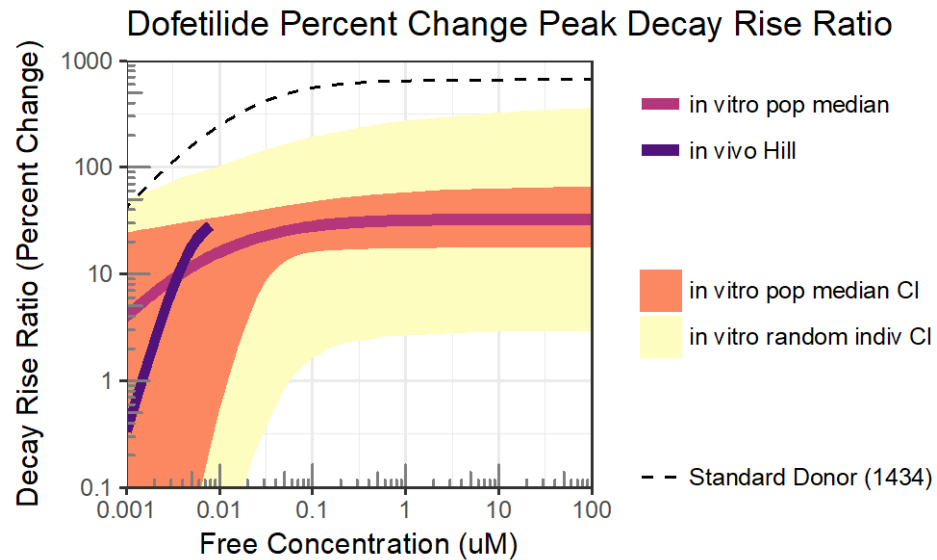


Figure S17. Comparison of dofetilide concentration-response functions based on *in vivo* data (purple line) compared to *in vitro* data (magenta line: population median; orange region: 95% confidence interval on population median; yellow region: 95% confidence interval on random individual; dashed line: standard iCell donor (1434).

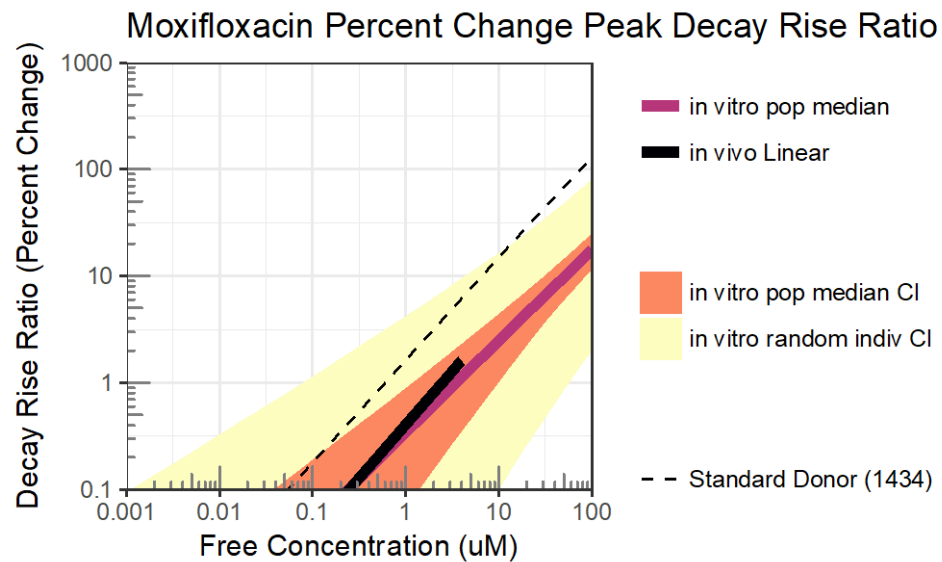


Figure S18. Comparison of moxifloxacin concentration-response functions based on *in vivo* data (black line) compared to *in vitro* data (magenta line: population median; orange region: 95% confidence interval on population median; yellow region: 95% confidence interval on random individual; dashed line: standard iCell donor (1434)).

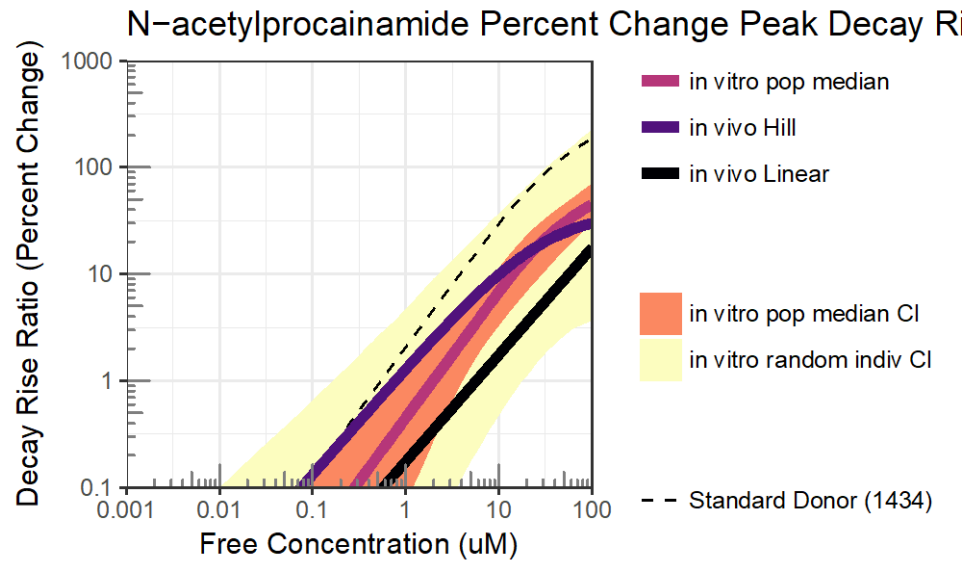


Figure S19. Comparison of n-acetylp procainamide concentration-response functions based on *in vivo* data (black line [linear], purple line [Hill]) compared to *in vitro* data (magenta line: population median; orange region: 95% confidence interval on population median; yellow region: 95% confidence interval on random individual; dashed line: standard iCell donor (1434)).

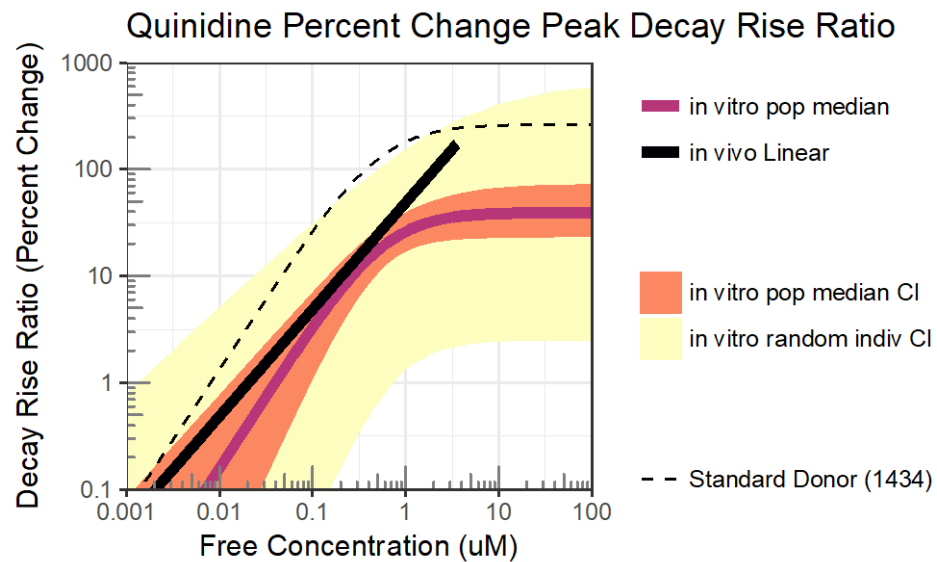


Figure S20. Comparison of quinidine concentration-response functions based on *in vivo* data (black line) compared to *in vitro* data (magenta line: population median; orange region: 95% confidence interval on population median; yellow region: 95% confidence interval on random individual; dashed line: standard iCell donor (1434)).

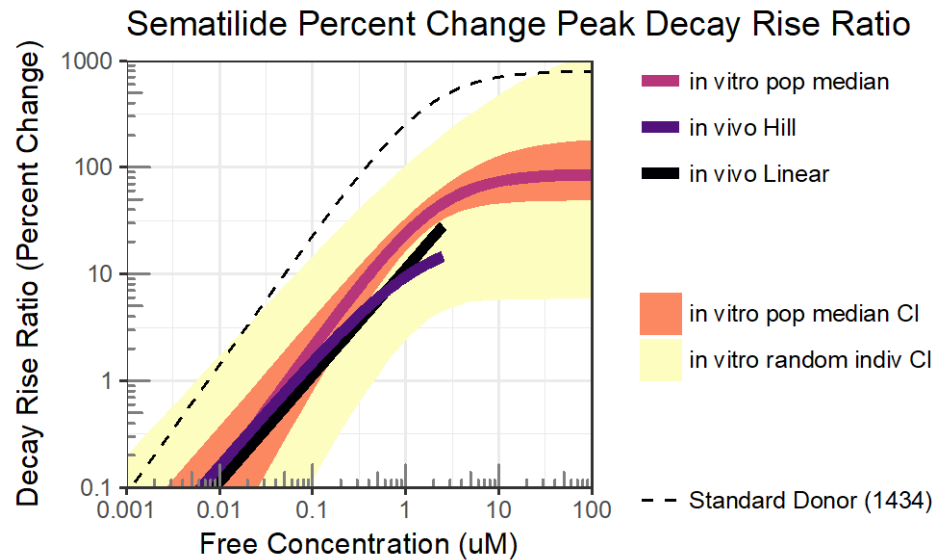


Figure S21. Comparison of sematilide concentration-response functions based on *in vivo* data (black line [linear] and purpose line [Hill]) compared to *in vitro* data (magenta line: population median; orange region: 95% confidence interval on population median; yellow region: 95% confidence interval on random individual; dashed line: standard iCell donor (1434)).

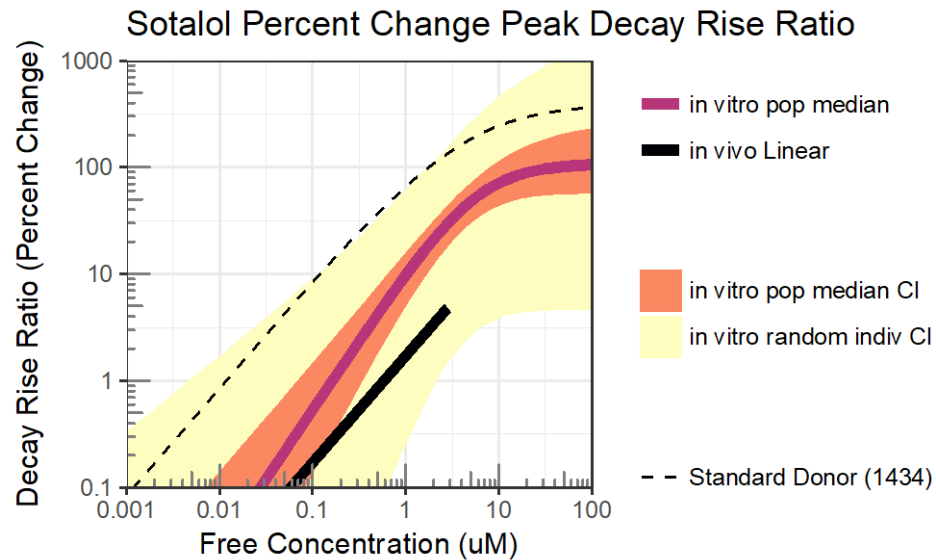


Figure S22 Comparison of sotalol concentration-response functions based on *in vivo* data (black line) compared to *in vitro* data (magenta line: population median; orange region: 95% confidence interval on population median; yellow region: 95% confidence interval on random individual; dashed line: standard iCell donor (1434)).

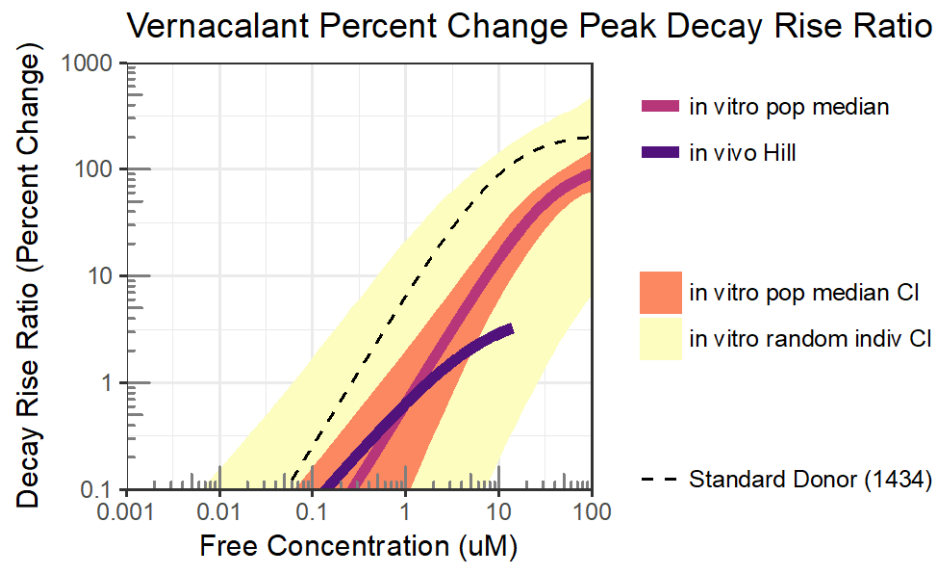


Figure S23. Comparison of vernacalant concentration-response functions based on *in vivo* data (purple line) compared to *in vitro* data (magenta line: population median; orange region: 95% confidence interval on population median; yellow region: 95% confidence interval on random individual; dashed line: standard iCell donor (1434).

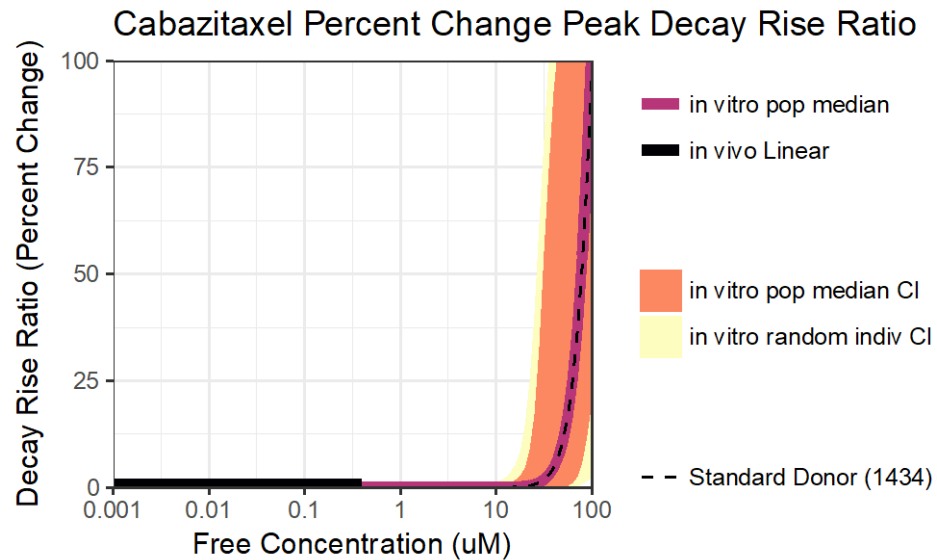


Figure S24. Comparison of cabazitaxel concentration-response functions based on *in vivo* data (black line) compared to *in vitro* data (magenta line: population median; orange region: 95% confidence interval on population median; yellow region: 95% confidence interval on random individual; dashed line: standard iCell donor (1434).

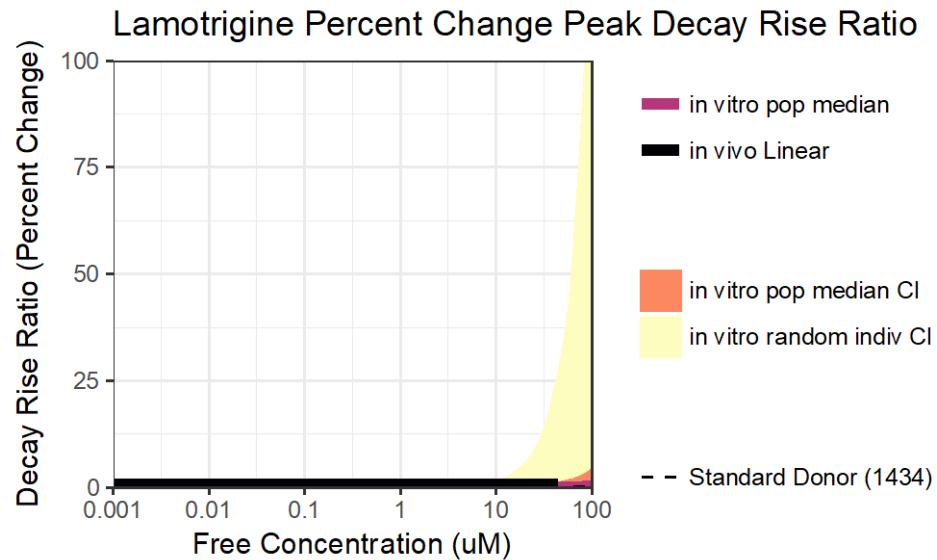


Figure S25. Comparison of lamotrigine concentration-response functions based on *in vivo* data (black line) compared to *in vitro* data (magenta line: population median; orange region: 95% confidence interval on population median; yellow region: 95% confidence interval on random individual; dashed line: standard iCell donor (1434).

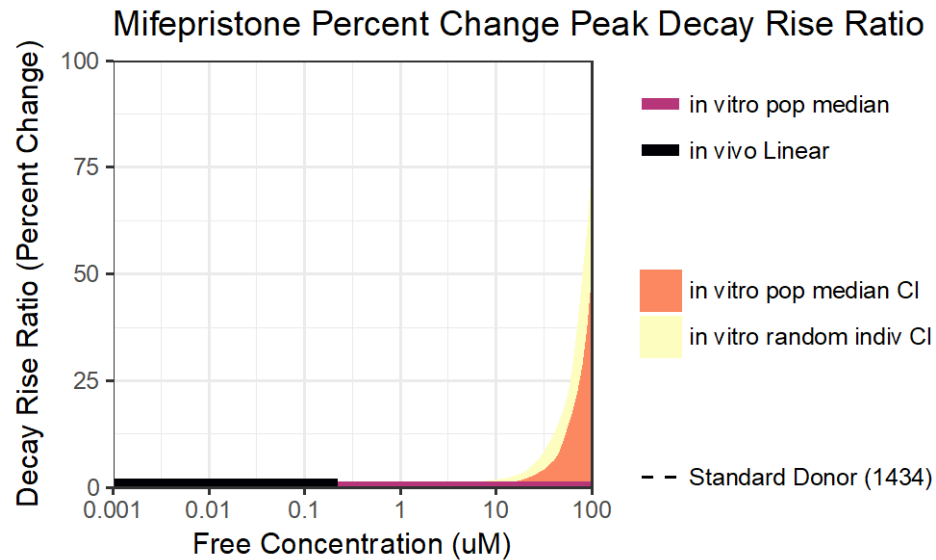


Figure S26. Comparison of mifepristone concentration-response functions based on *in vivo* data (black line) compared to *in vitro* data (magenta line: population median; orange region: 95% confidence interval on population median; yellow region: 95% confidence interval on random individual; dashed line: standard iCell donor (1434)).

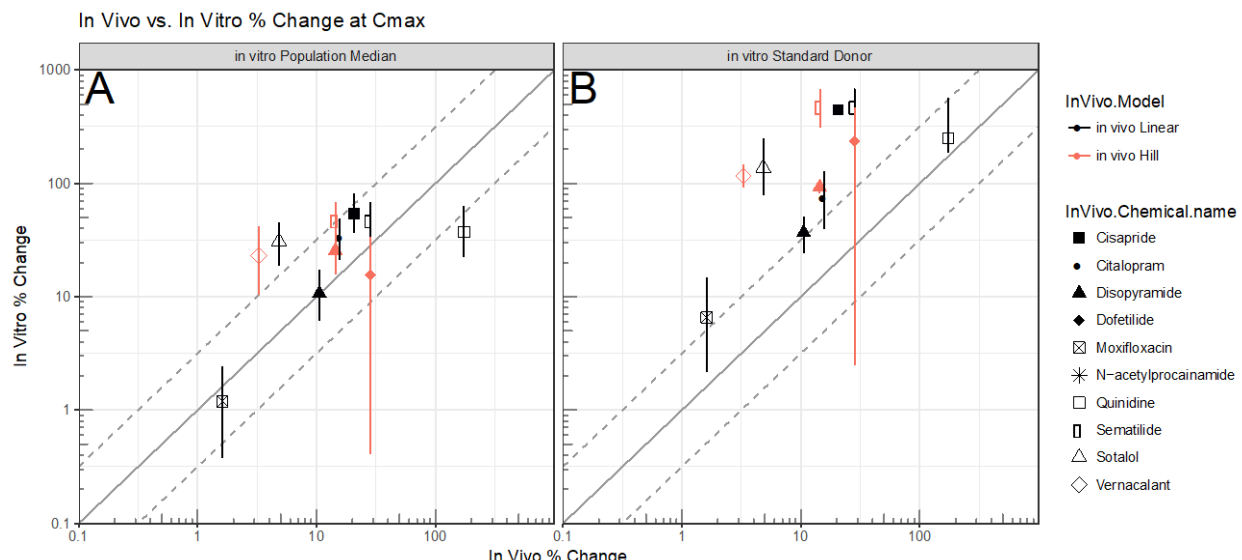


Figure S27. Comparison of *in vivo* response (% change) at Cmax with *in vitro* response (% change) at Cmax, based on (A) population median and (B) standard donor (1434).

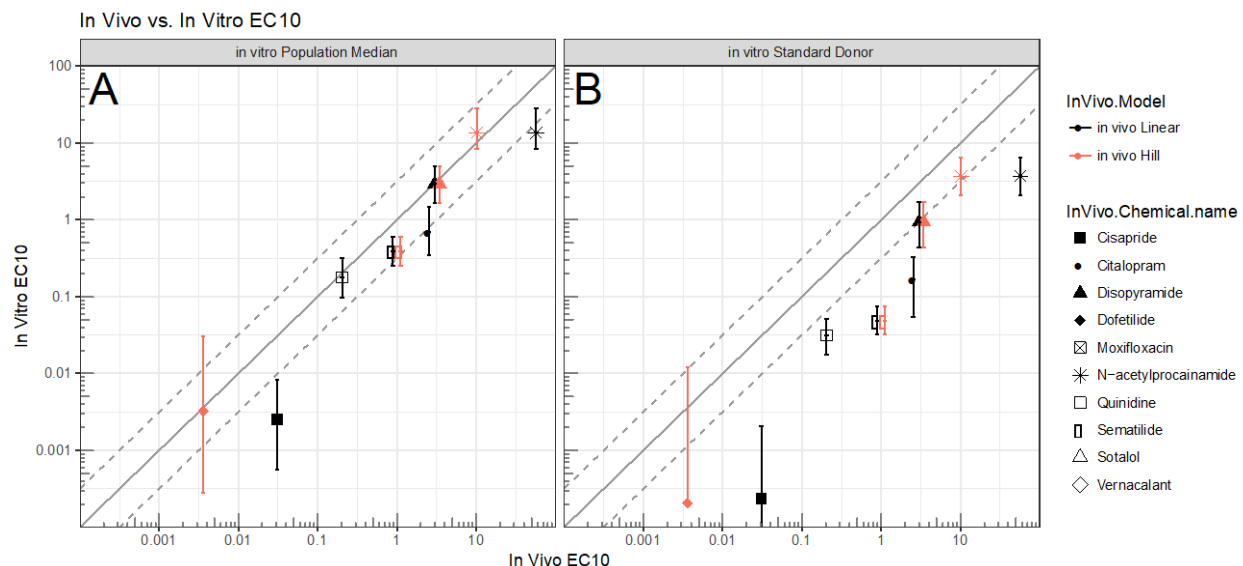


Figure S28. Comparison of *in vivo* EC₁₀ with *in vitro* EC₁₀, based on (A) population median and (B) standard donor (1434).

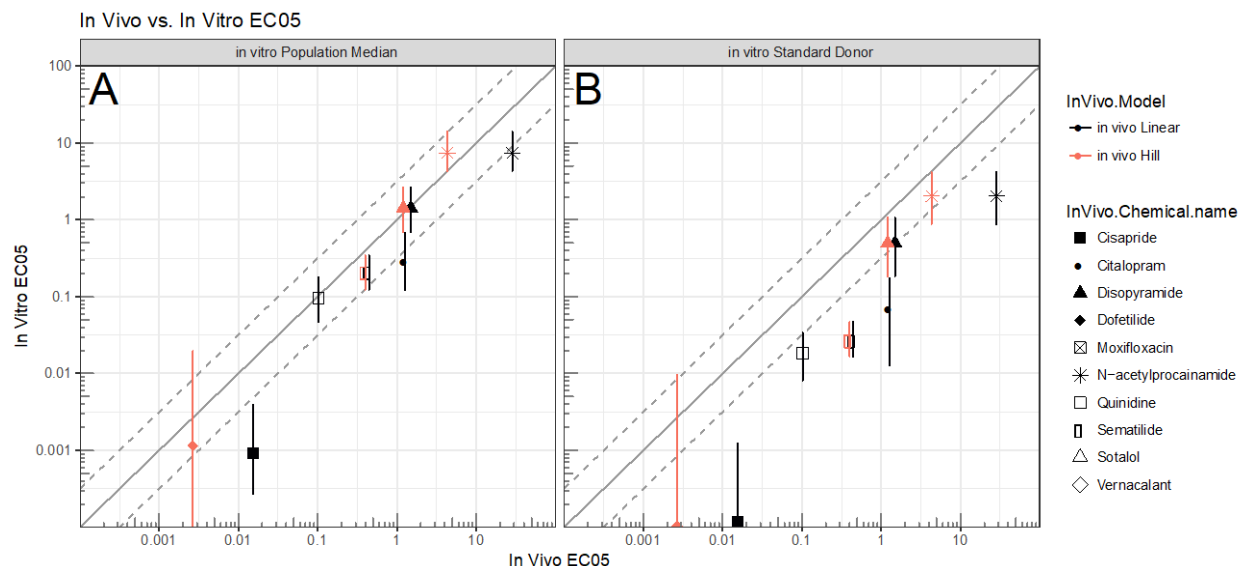


Figure S29. Comparison of *in vivo* EC₀₅ with *in vitro* EC₀₅, based on (A) population median and (B) standard donor (1434).

SUPPLEMENTAL TABLES

Table S1. Single Reaction Monitoring parameters for HPLC-MS/MS Analysis

Drug name	CAS #	MW	Molecular formula (analyte)	MW of interest	[M+H]	Mass transition (m/z)	C E
citalopram hydrobromide	59729-33-8	405.3	C ₂₀ H ₂₁ FN ₂ O	324.4	325.4	325→109	30
disopyramide phosphate	22059-60-5	437.5	C ₂₁ H ₂₉ N ₃ O	339.5	340.5	340→239	15
dofetilide	115256-11-6	441.6	C ₁₉ H ₂₇ N ₃ O ₅ S ₂	441.6	442.6	442→198	50
lamotrigine	84057-84-1	256.1	C ₉ H ₇ Cl ₂ N ₅	256.1	257.1	256→187	37
mifepristone	84371-65-3	429.6	C ₂₉ H ₃₅ NO ₂	429.6	430.6	430→372	35
moxifloxacin hydrochloride	186826-86-8	437.9	C ₂₁ H ₂₄ FN ₃ O ₄	401.4	402.4	402→358	19
n-acetylprocainamide	32795-44-1	277.4	C ₁₅ H ₂₃ N ₃ O ₂	277.4	278.4	278→205	18
quinidine sulfate	50-54-4	746.9	C ₂₀ H ₂₄ N ₂ O ₂	324.4	325.4	325→81	33
Sematilide	101526-83-4	313.4	C ₁₄ H ₂₃ N ₃ O ₃ S	313.4	314.4	314→162	37
sotalol hydrochloride	959-24-0	308.8	C ₁₂ H ₂₀ N ₂ O ₃ S	272.4	273.4	273→255	20
Vernakalant hydrochloride	748810-28-8	385.9	C ₂₀ H ₃₁ NO ₄	349.5	350.5	350→168	35
cisapride monohydrate	260779-88-2	484.0	C ₂₃ H ₂₉ ClFN ₃ O ₄	465.9	466.9	466→184	35
cabazitaxel	183133-96-2	835.9	C ₄₅ H ₅₇ NO ₁₄	835.9	836.9	836.6→555.5	13

ZORBAX SSHD Eclipse Plus C18 column (3.0 X 50 mm, 1.8 µm, catalogue #: 979757-302; Agilent, Santa Clara, CA) with a C18 guard column (2.1 X 5 mm, 1.8 µm, catalogue #: 821725-901; Agilent, Santa Clara, CA) were used for chromatography with the following solvent gradient [A: water with 0.1% formic acid; B: methanol with 0.1% formic acid, shown as Time (A%)]: 0(90)-1(90)-3(10)-4(2)-5(2)-5.2(90)-8(90).

Table S2. Plasma protein binding (free fraction) reported in literature

Drug	CAS N	Free fraction	References
Cisapride (monohydrate)	81098-60-4 (260779-88-2)	0.02-0.025 0.0395±0.037	(2, 3)
Citalopram (hydrobromide)	59729-33-8 (59729-32-7)	0.2	(4)
Disopyramide (phosphate)	3737-009-005 (22059-60-5)	0.25-0.50	(5)
Dofetilide	115256-11-6	0.17-0.337 (in all patients) 0.337±0.021 (in patients with normal kidney)	(6)
Moxifloxacin (hydrochloride)	151096-09-2 (186826-86-8)	0.3-0.5	(7)
N-acetylprocainamide	32795-44-1	0.3	(8)
Quinidine (sulfate)	56-54-2 (50-54-4)	0.1 0.12-0.2 (adult) 0.3-0.5 (pregnant) 0.77 0.23 (0.154-0.47)	(8-10)
Sematilide	101526-83-4	0.96	(11)
Sotalol (hydrochloride)	3930-20-9 (959-24-0)	1.0	(12)
Vernacularant (HCl)	794466-70-9 (748810-28-8)	0.53-0.63	(13)
Cabazitaxel	183133-96-2	0.05–0.066	(14, 15)
Lamotrigine	84057-84-1	0.45	(16)
Mifepristone	84371-65-3	0.01-0.02	(17, 18)

Table S3. Armitage et al. (2014)(19) model generic input parameters.

Test system parameters		Source	
384-well Cell Culture Plate		User-defined	
Size of surface area (cm ²)		User-defined	0.36
V _F	serum volume fraction in the bulk medium (L/L)	User-defined	0.05
C _D	Concentration of DOM (mg/L)	User-defined	0
D _D	Density of DOM (kg/L)	User-defined	1
C _{Sa}	Serum albumin concentration (g/L)	User-defined	21.65*
C _{Sl}	Serum lipid concentration (g/L)	User-defined	1.9
D _{Sa}	Density of serum albumin (kg/L)	User-defined	1.36
D _{Sl}	Density of serum lipids (kg/L)	User-defined	1
f _L	volume fraction of total lipid equivalent (i.e., pseudo-octanol content)	User-defined	0.05
D _C	Density (cells/mL)	User-defined	1
M _C	Mass (cells) (mg)	User-defined	3.0
C _S	Ionic strength of the medium (M)	User-defined	0.15
T _S	System temperature (C°)	User-defined	37
V _T	Total system volume	User-defined	0.149
V _M	Bulk medium (excluding cells/tissue) (Plating medium)	User-defined	0.05
V _A	volume of head space	Calculated	0.1
V _w	volume of medium (aqueous phase only)	Calculated	0.05
V _{Sa}	volume of serum albumin	Calculated	4.4E-05
V _{Sl}	volume of serum lipids	Calculated	4.8E-06
V _D	volume of DOM	Assumed	0
V _C	volume of cell/tissue (seeding volume)	User-defined	6.48E-5

Table S4. Armitage et al. (2014)(19) model chemical-specific input parameters.

Name	CAS	MW (g/mol)	MP (°C)	log K _{OW}					log K _{AW}	C _{SAT,W} (Sw) (mg/L)				
				log K _O w	Experi- mental	Mean	min	ma x		C _{SAT,W} (Sw) (mg/L)	Mean	min	max	Experi- mental
Cisapride	81098-60-4	466.0	261.5	3.09		3.19	3.02	3.65	-18.79	2.707	57.78	2.71	164.48	
Citalopram hydrobromide	59729-32-7	405.3	188.0	2.92		2.92	2.51	3.39	-7.68	19.04	137.8	8.471	380.58	
Citalopram	59729-33-8	324.4	188.0	3.74		3.08	2.51	3.74	-8.96	31.09	90.505	6.78	304.6	
Disopyramide	3737-09-05	339.5	94.8	2.58		2.60	1.70	2.96	-13.98	44.882	20.776	0.128	44.81	
Dofetilide	11525-6-11-6	441.6	251.37	2.14		1.57	0.12	2.33	-13.37	256.3	166.47	44.156	289.6634	
Moxifloxacin	15109-6-09-2	401.4	325.0	0.95		1.17	0.08	2.43	-17.90	11467	355.667	5.820735	1144.076	
Moxifloxacin hydrochloride	18682-6-86-8	437.9	325.0	1.22		1.22	0.08	2.43	-8.35	7.81	100.7147	6.349405	287.2558	
N-acetylprocainamide	32795-44-1	277.4	210.1	0.99		1.27	0.99	1.53	-12.38	236776	7183.676	926.3891	24407.86	
Quinidine	56-54-2	324.0	189.5	3.44		2.86	1.57	3.44	-13.46	140	216.1	152.604	261.468	2.64E+02
Sematilide	10152-6-83-4	313.4	208.3	1.36		1.09	0.92	1.24	-13.30	12281	3886.41	91.83206	13069.6	
Sotalol	3930-20-9	272.4	207	0.24		0.24	-0.33	0.55	-12.00	876.455	5637.85	876.9992	14544.02	5510
Vernakalant	79446-6-70-9	349.5	178.03	2.64		2.80	2.17	4.07	-12.47	350.6	124058.3	313.472	496233.2	
Cabazitaxel	18313-3-96-2	835.9	182	4.31		4.31	2.24	7.56	-5.29	6.08	44.054	0.0024	167.19	

Lamotrigine	84057-84-1	256.0	189.2	0.9	2.57	1.19	-0.19	2.5	-9.04	3127	10675.2	17.92	39424	
Mifepristone	84371-65-3	429.6	230.2	5.3		5.05	4.70	5.3	-9.04	33	33.42	0.0498	91.93	

Data from ChemSpider and U.S. EPA Chemistry Dashboard.

Table S5. Clinical *in vivo* PK-PD models for QTc prolongation.

Drug treatment	Free fraction in plasma [1]	Free fraction in media [1]	In Vivo Model Type[2]	QTc0 (msec)	Other parameters[3]	Cmax (uM Free)	Reference
[1]							
<i>Positive for clinical QTc prolongation in “healthy” population</i>							
Cisapride	0.072	0.616	Linear	386	Slope = 1260	0.067	(20)
Citalopram hydrobromide	0.773	1.000	Linear	425	Slope = 16.8	4.3	(21)
Disopyramide phosphate	0.671	0.954	Linear	450	Slope = 15.0	3.2	(22)
			Hill	450	Emax = 97.4; n = 1; Kd = 2.69		(23)
Dofetilide	0.622	0.864	Hill	368	Emax = 131; n = 2.9; Kd = 0.0031	0.0085	(24)
Moxifloxacin hydrochloride	1.000	0.934	Linear	396	Slope = 1.61	4.4	(25)
N-acetyl procainamide	0.978	0.965	Linear	440	Slope = 0.770	112	(26)
			Hill	440	Emax = 170; n = 1; Kd = 28.5	112	
Quinidine sulfate	0.375	0.675	Linear	407	Slope = 199	3.8	(27)
Sematilide	0.847	0.955	Linear	394	Slope = 44.3	2.6	(11)
			Hill	394	Emax = 90.5; n = 1; Kd = 1.22	2.6	
Sotalol	0.920	0.968	Linear	380	Slope = 6.51	3.1	(25)
Vernacalant	0.788	0.966	Hill	424	Emax = 20.3; n = 1; Kd = 5.14	15	(28)
<i>Negative for clinical QTc prolongation in “healthy” population [4]</i>							
Cabazitaxel	0.204	0.705	Linear	400	Slope = 0	0.44	(29)
Lamotrigine	0.872	1.000	Linear	400	Slope = 0	48	(30)
Mifepristone	0.017	0.583	Linear	400	Slope = 0	0.24	(31)

[1]See Main Text Table 1. Measured values >1 were set to 1.

[2]Model formulas: linear ($QTc = QTc0 + Slope \times C_{free}$) and Hill ($QTc = QTc0 + Emax \times C_{free}^n / (Kd^n + C_{free}^n)$)

[3]Units of other model parameters: Slope (msec/uM free), Emax (msec), Kd (uM free)

[4]Slope set to zero for negative controls

SUPPLEMENTAL REFERENCES

- (1) Carpenter, B. *et al.* Stan: A Probabilistic Programming Language. *J Stat Softw* **76**, 1-32 (2017).
- (2) U.S.FDA. FDA approval package: Cisapride monohydrate. (ed. Research, C.f.D.E.a.) 7 (2000).
- (3) U.S.FDA. FDA approval package: Biopharmaceutical review: Cisapride. (ed. Biopharmaceutics, D.o.) A17 (1992).
- (4) U.S.FDA. FDA package: Citalopram hydrobromide. 3 (2009).
- (5) U.S.FDA. FDA approval package: Disopyramide phosphate. 15 (1982).
- (6) U.S.FDA. FDA approval package: Biopharmaceutical review: Dofetilide Vol. 1.28 127 (1998).
- (7) U.S.FDA. FDA approval package: Moxifloxacin hydrochloride. 4 (2009).
- (8) Valkó, K.L., Nunhuck, S.B. & Hill, A.P. Estimating Unbound Volume of Distribution and Tissue Binding by In Vitro HPLC-Based Human Serum Albumin and Immobilised Artificial Membrane-Binding Measurements. *Journal of Pharmaceutical Sciences* **100**, 849-62 (2011).
- (9) U.S.FDA. FDA approval package: Quinidine sulfate. (ed. Research, C.f.D.E.a.) 12 (1989).
- (10) U.S.FDA. FDA approval package: Quinidine sulfate. 1 (2000).
- (11) Shi, J., Lasser, T., Koziol, T. & Hinderling, P.H. Kinetics and dynamics of sematilide. *Ther Drug Monit* **17**, 437-44 (1995).
- (12) U.S.FDA. FDA approval package: Sotalol hydrochloride. 3 (1992).
- (13) EMEA. Assessment report: Vernakalant. (ed. Agency, E.M.) 15 (2011).
- (14) Azaro, A. *et al.* A phase I pharmacokinetic and safety study of cabazitaxel in adult cancer patients with normal and impaired renal function. *Cancer Chemotherapy and Pharmacology* **78**, 1185-97 (2016).
- (15) Sarantopoulos, J. *et al.* Safety and pharmacokinetics of cabazitaxel in patients with hepatic impairment: a phase I dose-escalation study. *Cancer Chemotherapy and Pharmacology* **79**, 339-51 (2017).
- (16) Patsalos, P.N., Zugman, M., Lake, C., James, A., Ratnaraj, N. & Sander, J.W. Serum protein binding of 25 antiepileptic drugs in a routine clinical setting: A comparison of free non-protein-bound concentrations. *Epilepsia* **58**, 1234-43 (2017).
- (17) U.S.FDA. FDA approval package: Mifepristone (ed. Research, C.f.D.E.a.) 11 (2016).
- (18) U.S.FDA. FDA approval package: Mifepristone. 7 (2012).
- (19) Armitage, J.M., Wania, F. & Arnot, J.A. Application of mass balance models and the chemical activity concept to facilitate the use of in vitro toxicity data for risk assessment. *Environ Sci Technol* **48**, 9770-9 (2014).
- (20) Chain, A.S., Dubois, V.F., Danhof, M., Sturkenboom, M.C. & Della Pasqua, O. Identifying the translational gap in the evaluation of drug-induced QTc interval prolongation. *British journal of clinical pharmacology* **76**, 708-24 (2013).
- (21) Friberg, L.E., Isbister, G.K. & Duffull, S.B. Pharmacokinetic-pharmacodynamic modelling of QT interval prolongation following citalopram overdoses. *British journal of clinical pharmacology* **61**, 177-90 (2006).
- (22) Thibonnier, M., Holford, N.H., Upton, R.A., Blume, C.D. & Williams, R.L. Pharmacokinetic-pharmacodynamic analysis of unbound disopyramide directly measured

- in serial plasma samples in man. *Journal of pharmacokinetics and biopharmaceutics* **12**, 559-73 (1984).
- (23) Lima, J.J. & Boudoulas, H. Stereoselective effects of disopyramide enantiomers in humans. *Journal of cardiovascular pharmacology* **9**, 594-600 (1987).
- (24) Le Coz, F., Funck-Brentano, C., Morell, T., Ghadanfar, M.M. & Jaillon, P. Pharmacokinetic and pharmacodynamic modeling of the effects of oral and intravenous administrations of dofetilide on ventricular repolarization. *Clin Pharmacol Ther* **57**, 533-42 (1995).
- (25) Chain, A.S., Krudys, K.M., Danhof, M. & Della Pasqua, O. Assessing the probability of drug-induced QTc-interval prolongation during clinical drug development. *Clin Pharmacol Ther* **90**, 867-75 (2011).
- (26) Piergies, A.A., Ruo, T.I., Jansyn, E.M., Belknap, S.M. & Atkinson, A.J., Jr. Effect kinetics of N-acetylprocainamide-induced QT interval prolongation. *Clin Pharmacol Ther* **42**, 107-12 (1987).
- (27) Karbwang, J., Davis, T.M., Looareesuwan, S., Molunto, P., Bunnag, D. & White, N.J. A comparison of the pharmacokinetic and pharmacodynamic properties of quinine and quinidine in healthy Thai males. *British journal of clinical pharmacology* **35**, 265-71 (1993).
- (28) Mao, Z., Wheeler, J.J., Townsend, R., Gao, Y., Kshirsagar, S. & Keirns, J.J. Population pharmacokinetic-pharmacodynamic analysis of vernakalant hydrochloride injection (RSD1235) in atrial fibrillation or atrial flutter. *J Pharmacokinet Pharmacodyn* **38**, 541-62 (2011).
- (29) Maison-Blanche, P. *et al.* An open-label study to investigate the cardiac safety profile of cabazitaxel in patients with advanced solid tumors. *Cancer chemotherapy and pharmacology* **73**, 1241-52 (2014).
- (30) Dixon, R. *et al.* Lamotrigine does not prolong QTc in a thorough QT/QTc study in healthy subjects. *British journal of clinical pharmacology* **66**, 396-404 (2008).
- (31) Darpo, B., Bullingham, R., Combs, D.L., Ferber, G. & Hafez, K. Assessment of the cardiac safety and pharmacokinetics of a short course, twice daily dose of orally-administered mifepristone in healthy male subjects. *Cardiology journal* **20**, 152-60 (2013).